Arx homeobox gene is essential for development of mouse olfactory system

Sei-ichi Yoshihara[1], Kayo Omichi[2], Masako Yanazawa[2], Kunio Kitamura[2,*,†] and Yoshihiro Yoshihara[1,†]

[1]Laboratory for Neurobiology of Synapse, RIKEN Brain Science Institute, Wako-shi, Saitama 351-0198, Japan
[2]Mitsubishi Kagaku Institute of Life Sciences, Machida-shi, Tokyo 194-8511, Japan
*Present address: Department of Mental Retardation and Birth Defect Research, National Institute of Neuroscience, National Center of Neurology and Psychiatry, 4-1-1 Ogawahigashi, Kodaira, Tokyo 187-8502, Japan
†Authors for correspondence (e-mail: yoshihara@brain.riken.go.jp or kitamura@ncnp.go.jp)

Accepted 15 December 2004

Development 132, 751-762
Published by The Company of Biologists 2005
doi:10.1242/dev.01619

Summary

The olfactory system provides an excellent model in which to study cell proliferation, migration, differentiation, axon guidance, dendritic morphogenesis, and synapse formation. We report here crucial roles of the *Arx* homeobox gene in the developing olfactory system by analyzing its mutant phenotypes. Arx protein was expressed strongly in the interneurons and weakly in the radial glia of the olfactory bulb, but in neither the olfactory sensory neurons nor bulbar projection neurons. *Arx*-deficient mice showed severe anatomical abnormalities in the developing olfactory system: (1) size reduction of the olfactory bulb, (2) reduced proliferation and impaired entry into the olfactory bulb of interneuron progenitors, (3) loss of tyrosine hydroxylase-positive periglomerular cells, (4) disorganization of the layer structure of the olfactory bulb, and (5) abnormal axonal termination of olfactory sensory neurons in an unusual axon-tangled structure, the fibrocellular mass. Thus, *Arx* is required for not only the proper developmental processes of *Arx*-expressing interneurons, but also the establishment of functional olfactory neural circuitry by affecting *Arx*-non-expressing sensory neurons and projection neurons. These findings suggest a likely role of *Arx* in regulating the expression of putative instructive signals produced in the olfactory bulb for the proper innervation of olfactory sensory axons.

Key words: Arx, Olfactory bulb, Granule cells, Periglomerular cells, Rostral migratory stream, Radial glia, Olfactory axons, Axon guidance, Fibrocellular mass, Mouse

Introduction

Arx/ARX is the vertebrate X-linked *prd*-type homeobox gene closely related to the *Drosophila* gene *aristaless*. *Arx* is expressed in the forebrain, floor plate, testis, and pancreas of embryonic mice (Miura et al., 1997; Collombat et al., 2003). In the human, *ARX* mutation is associated with X-linked lissencephaly with abnormal genitalia (XLAG) (Kitamura et al., 2002), X-linked mental retardation (XLMR) (Bienvenu et al., 2002; Stromme et al., 2002), and X-linked myoclonic epilepsy with spasticity and intellectual disability (XMESID) (Scheffer et al., 2002). We previously demonstrated that disruption of the *Arx* gene causes aberrant migration and differentiation of GABAergic interneuron progenitors from the ganglionic eminence to the cerebral neocortex (Kitamura et al., 2002). In addition, we noticed that *Arx*-deficient newborn mice have smaller a olfactory bulb (OB) compared to wild-type (Kitamura et al., 2002).

The OB is the first relay station in the olfactory system, where odor information is transferred from the periphery to higher centers in the brain (Mori et al., 1999). It comprises limited types of neurons and glia with a simple layer organization. Outermost is the olfactory nerve layer (ONL) consisting of olfactory axons projecting from the olfactory epithelium (OE) and olfactory ensheathing glia that enwrap these axons. Beneath the ONL lies the glomerular layer (GL) where olfactory axons make synapses in glomeruli with primary dendrites of projection neurons and dendrites of interneurons. Projection neurons in the OB are mitral and tufted cells whose cell bodies are situated in the mitral cell layer (MCL) and the external plexiform layer, respectively. In addition, the external plexiform layer contains secondary dendrites of mitral and tufted cells that make dendrodendritic synapses with spines of granule cells. Local interneurons in the OB are classified into two major types: periglomerular cells and granule cells. Somata of periglomerular cells are localized around glomeruli, while those of granule cells are mostly found in the granule cell layer (GCL).

OB projection neurons and interneurons are destined in different ways. The projection neurons are born earlier than the interneurons (Hinds, 1968). This time difference of neurogenesis results in two steps of OB morphogenesis: the first step as a slight evagination of primordial OB at the anterior tip of the telencephalon by accumulation of differentiated projection neurons [embryonic day 12-13 (E12-13) in mice] and the second step as a further expansion by massive addition of differentiated interneurons (E14-18 in mice). In addition, the most striking difference is that the interneurons are continuously generated throughout the animal's life. Their

progenitors are born in the subventricular zone (SVZ) of the cerebral cortex and migrate toward the OB via the rostral migratory stream (RMS) (Luskin, 1998).

Here, we analyzed olfactory system development in *Arx*-deficient mice. *Arx* mutation resulted in the impaired entry of interneuron progenitors into the OB and the disruption of OB layer organization. In addition, most of the olfactory axons failed to reach the OB and formed a tangle-like structure between the OE and OB, although Arx is not expressed in the olfactory sensory neurons. These observations suggest that *Arx* is essential for development of the olfactory system and that the proper projection of olfactory axons depends on the normal development of the OB.

Materials and methods

Animals and tissue preparation

Mice with targeted disruption of the *Arx* gene were previously described (Kitamura et al., 2002). Because *Arx*-deficient mice die soon after birth, our analysis is limited to embryonic development. For staging of embryos, the day of vaginal plug was considered as day 0 of embryonic development (E0). Embryos were collected from pregnant mice by Cesarean section. Genotypes were determined by PCR. Since the *Arx* gene is located on the X chromosome, *Arx* hemizygous mutant male mice were used as *Arx*-deficient mice in this study. E11.5-E14.5 embryos were immersion-fixed in 4% paraformaldehyde (PFA) in PBS at 4°C for 2 hours. E16.5 to postnatal day 60 (P60) animals were transcardially perfused with 4% PFA in PBS and postfixed in the same fixative at 4°C for 2 hours. Samples were cryoprotected in 30% sucrose, frozen in embedding medium (OCT; Tissue-Tek), and sectioned using a cryostat at 10 μm.

Production of polyclonal antibodies against Tbx21

In the brain, a T-box transcription factor, Tbx21, is specifically expressed in mitral/tufted cells (Faedo et al., 2002). To obtain a good immunohistochemical marker, we generated polyclonal antibodies against Tbx21. A peptide corresponding to the carboxyl-terminal 20 amino acids (GAPSPFDKETEGQFYNYFPN) of mouse Tbx21 was synthesized, coupled to keyhole limpet hemocyanin, and used to immunize rabbits and guinea pigs. The antisera showed specific labeling of the mitral/tufted cells.

Histology and immunohistochemistry

Nissl staining was performed as described previously (Long et al., 2003). Images were obtained with an upright light microscope equipped with a cooled CCD digital camera (Olympus AX80, DP50).

Immunohistochemistry was performed essentially as described previously (Yoshihara et al., 1997). Sections were blocked with PBS containing 10% normal horse serum, incubated with primary antibodies overnight at 4°C, washed, and incubated with Cy3-, Cy5- (Jackson ImmunoResearch Laboratories) or Alexa488- (Molecular Probes) labeled secondary antibodies. All secondary antibodies were used at 1:300 dilution. Antigen retrieval pretreatment with a microwave oven (550 W, 5 minutes) greatly enhanced the immunoreactivity of Arx protein. The following primary antibodies were used: Arx (rabbit, 1:1000) (Kitamura et al., 2002), DCC (goat, 1:100; Santa Cruz Biotechnology), Eph-A4 (goat, 1:100; R&D Systems), Eph-B1 (goat, 1:50, R&D Systems), Eph-B2 (goat, 1:50, R&D Systems), Eph-B3 (goat, 1:50, R&D Systems), ephrin-B2 (goat, 1:50, R&D Systems), ephrin-B3 (goat, 1:50, R&D Systems), GABA (rabbit, 1:2000; Sigma) (rat, 1:400; Affiniti Research Products), GLAST (guinea pig, 1:8000; Chemicon), α1 integrin (rabbit, 1:1000; Chemicon), β1 integrin (rat, 1:50; BD Pharmingen), β8 integrin (goat, 1:100; Santa Cruz Biotechnology), L1 (rat, 1:200; Chemicon), LacZ (rabbit, 1:300; 5Prime 3Prime Inc.), NCAM (rat, 1:500; Chemicon), neuropeptide Y (rabbit, 1:3000; Incstar), neuropilin-1 (goat, 1:200; R&D Systems), neuropilin-2 (goat, 1:200; R&D Systems), OCAM (rabbit, 1:1000) (Yoshihara et al., 1997), olfactory marker protein (OMP) (goat, 1:20000; provided by F. Margolis) (Keller and Margolis, 1975), PSA-NCAM (mouse, 1:500; provided by T. Seki), (Seki and Arai, 1993), Rig1 (rabbit, 1:1500), Robo1 (rabbit, 1:1500), Robo2 (rabbit, 1:1500) (anti-Rig1, -Robo1, -Robo2 antibodies were provided by F. Murakami and A. Tamada) (Sabatier et al., 2004), Reelin (CR-50) (mouse, 1:200; provided by M. Ogawa) (Ogawa et al., 1995) S100 (rabbit, 1:5000; Dako), Tbx21 (rabbit, 1:10000; guinea pig, 1:25000), Thy-1 (rat, 1:200; Santa Cruz Biotechnology), tyrosine hydroxylase (TH) (mouse, 1:200; Chemicon). Images of immunofluorescently labeled sections were obtained with a fluorescent microscope (Zeiss AxioPlan2) equipped with a cooled CCD camera (Olympus DP70) or confocal laser scanning microscopes (BioRad MicroRadiance and Leica TCS SP2). All images were analyzed with Adobe Photoshop 6.0 software (Adobe Systems).

In situ hybridization

In situ hybridization was performed using digoxigenin (DIG)-labeled cRNA probes as described previously (Tsuboi et al., 1999). The following probes were used: *Dlx2* (nucleotides 317-1051, GenBank NM_010054), *Dlx5* (nucleotides 211-959, GenBank NM_010056), and *Nurr1* probe (nucleotides 340-1147, GenBank S53744). These probes were obtained by RT-PCR from brain RNA of newborn mice. Hybridization signals were detected with alkaline phosphatase-conjugated anti-DIG Fab fragments (1:1000; Roche Applied Science), followed by color development with NBT and BCIP (Roche Applied Science). All images were captured with a cooled CCD camera (Olympus DP50) on a light microscope (Olympus AX80).

BrdU labeling

BrdU labeling was performed as described previously (Kitamura et al., 2002). Pregnant mice were injected intraperitoneally with BrdU (40 mg/kg) and killed either after 1 hour or at P0. For proliferation analysis, 10 μm serial coronal sections were prepared form the anterior tip of the OB to the medial ganglionic eminence of E14.5 wild-type and mutant mice, and stained with anti-BrdU antibody (rat, 1:50; Oxford Biotechnology). BrdU(+) cells in every ten sections were counted (n=3 for each genotype).

Results

Arx is expressed in local interneurons and radial glia of OB

To characterize Arx expression in the developing olfactory system, we performed immunohistochemistry using anti-Arx antibody on parasagittal sections of wild-type mouse heads. At E11.5, Arx protein was strongly expressed in the mantle and intermediate zones of the ganglionic eminence (Fig. 1A), consistent with our previous in situ hybridization result (Miura et al., 1997). A similar pattern of Arx expression was observed at E12.5 when the primordial OB was first detectable as a slight evagination at the tip of telencephalon (Fig. 1B). At E14.5 when the protrusion of the OB became evident, Arx was intensely expressed in migrating cells within the RMS, some of which had already reached the OB (Fig. 1C). At E16.5 when a massive addition of OB interneurons from the RMS was taking place, Arx was present in presumptive GCL and GL of the OB as well as in the RMS (Fig. 1D). At P0 when the layer organization of OB became obvious, a robust expression of Arx was detected in the GCL and GL (Fig. 1E). Thereafter, Arx expression in the GCL and GL persisted toward adulthood (Fig. 1F). It is noteworthy that Arx expression was confined

exclusively within the brain and was not detected in the OE and vomeronasal organ at any developmental stages (Fig. 1A-F).

To identify Arx-expressing cells, we performed double or triple immunofluorescence labeling of OB coronal sections at P0. Tbx21 is specifically expressed in OB projection neurons, mitral/tufted cells (Faedo et al., 2002). Anti-Tbx21 labeling clearly demarcated the MCL at P0 (Fig. 1H). Arx immunoreactivity did not overlap with Tbx21, suggesting the absence of Arx in OB projection neurons (Fig. 1G-J). Also at earlier stages (E12.5, E16.5), Arx was not expressed in OB projection neurons (Fig. S1 in the supplementary material).

There are two major types of GABAergic interneurons in the OB: periglomerular cells and granule cells. In addition, a subpopulation of periglomerular cells also expresses catecholamine-synthesizing enzyme, TH (Kosaka et al., 1995). Arx immunoreactivity markedly overlapped with GABA(+) profiles in both the GL and GCL (Fig. 1K-V). In the GL, colocalization of Arx, GABA, and TH was observed, and the TH(+) periglomerular cells were always positive for Arx and GABA (Fig. 1K-R, arrowheads). In the GCL, a significant population of cells was positive only for Arx, but not GABA, probably corresponding to immature GCs (Fig. 1K-N,S-V).

Glutamate transporter GLAST is expressed in radial glia (Hartfuss et al., 2001). A weak but significant expression of Arx was detected in GLAST(+) radial glia (Fig. 1S-V, arrowheads). These results demonstrate that Arx is strongly expressed in the GABA(+) and TH(+) local interneurons and weakly in the GLAST(+) radial glia, but not in the Tbx21(+) projection neurons, in developing OB.

Failure of OB morphogenesis in *Arx*-deficient mice

We previously noticed that *Arx*-deficient mice had a smaller OB than wild-type mice (Kitamura et al., 2002). Here we made extensive analyses on abnormalities in the olfactory system caused by mutation of the *Arx* gene. First, we examined gross morphology of the developing OB. At E12.5, no apparent difference was observed in the telencephalic structure between wild-type (Fig. 2A) and *Arx*-deficient mice (Fig. 2B). At E16.5, the formation of the OB was evident as a protrusion from the anterior tip of telencephalon in wild-type mice (Fig. 2C). In contrast, only a slight protrusion of presumptive OB was detectable in mutant mice (Fig. 2D). At P0, the OB of the mutant mouse (Fig. 2F) was much smaller than that of wild-type mice (Fig. 2E). In addition, there was a wide empty space between

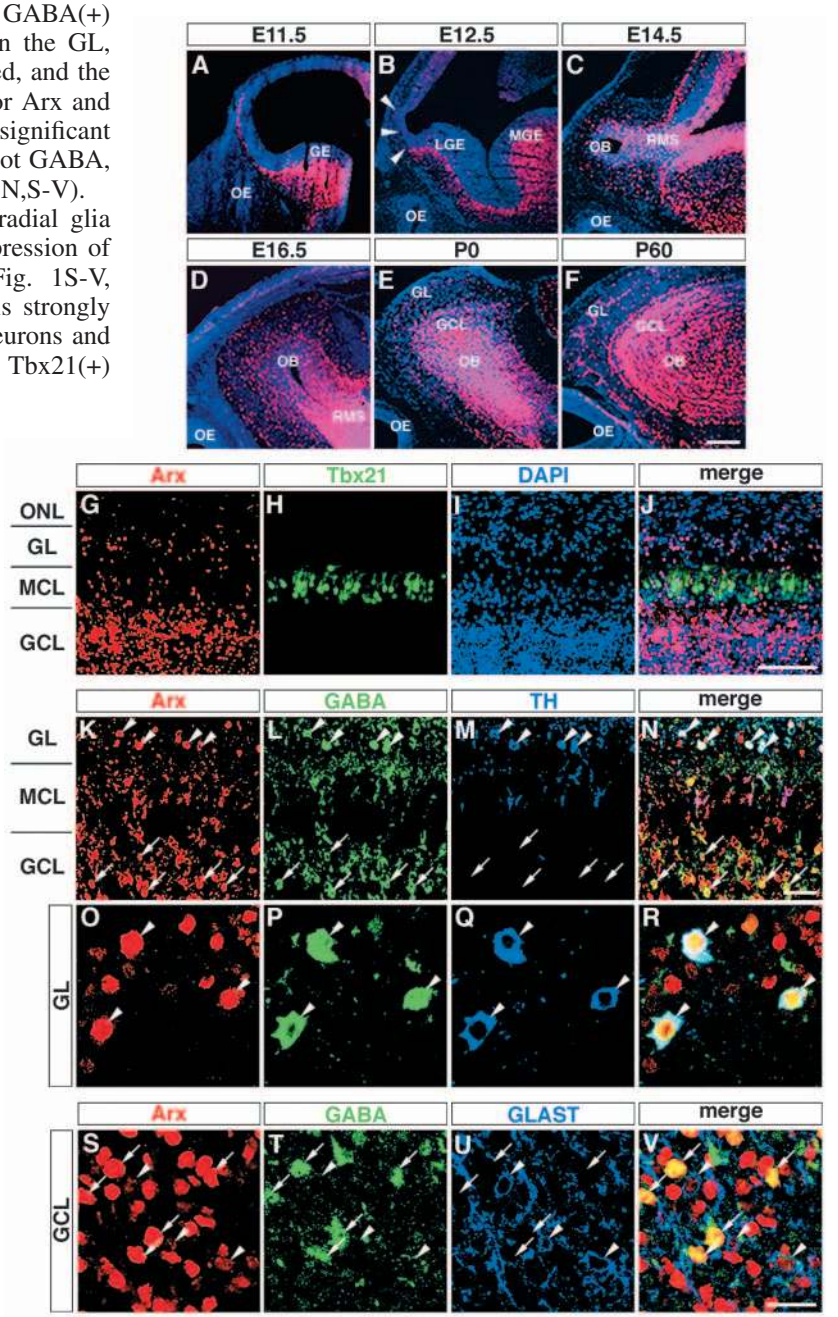

Fig. 1. Expression of Arx in developing mouse OB. Parasagittal sections of E11.5 (A), E12.5 (B), E14.5 (C), E16.5 (D), P0 (E), and P60 (F) wild-type mice were labeled with anti-Arx antibody (red) and counterstained with PI (blue: nucleus). Note that Arx is expressed in the olfactory bulb (OB) and rostral migratory stream (RMS), but not in olfactory epithelium (OE), at all the stages. Arrowheads in B: OB anlagen. Signals in the OE at P60 are non-specific autofluorescence (F). (G-V) Coronal sections of P0 wild-type mouse OB. (G-J) A triple-labeled section for Arx (red in G,J), Tbx21 (green in H,J: mitral cells), and DAPI (blue in I,J: nucleus). Arx is not expressed in Tbx21(+) mitral cells. (K-R) A triple-labeled section for Arx (red in K,N,O,R), GABA (green in L,N,P,R), and TH (blue in M,N,Q,R). (O-R) A magnified view of the glomerular layer (GL). Arrowheads in (K-R): Arx(+), GABA(+), and TH(+) periglomerular cells in the GL. Arrows in (K-N): Arx(+) and GABA(+) granule cells in the granule cell layer (GCL). (S-V) A magnified view of the GCL. A triple-labeled section for Arx (red in S,V), GABA (green in T,V: granule cells), and GLAST (blue in U,V: radial glia). Arrows in (S-V): Arx(+) and GABA(+) granule cells. Arrowheads in (S-V): Arx(+) and GLAST(+) radial glia. GE, ganglionic eminence; LGE, lateral ganglionic eminence; MCL, mitral cell layer; MGE, medial ganglionic eminence; ONL, olfactory nerve layer. Scale bars: in F, 200 μm for A-F; in J, 100 μm for G-J; in N, 40 μm for K-N; in V, 20 μm for O-V.

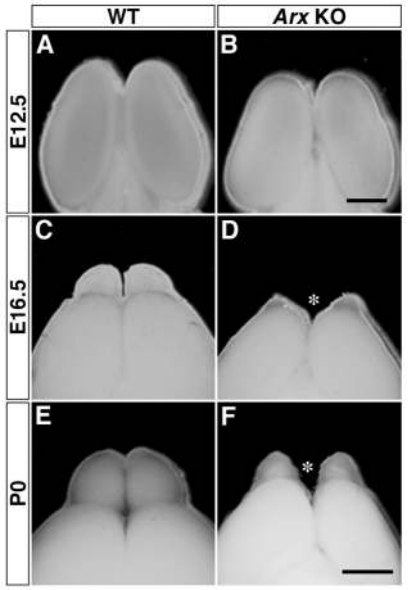

Fig. 2. Failure of OB morphogenesis in *Arx*-deficient mice. Whole-mount dorsal views of the anterior telencephalon at E12.5 (A,B), E16.5 (C,D), and P0 (E,F). At E12.5, the anterior telencephalon was indistinguishable between *Arx*-deficient (B) and wild-type (A) mice. At E16.5 and P0, mutant OB (D,F) was smaller than wild-type OB (C,E). Note that there is a wide empty space between the left and right OB of mutant mouse (asterisks in D,F). Scale bars: in B, 500 μm for A,B; in F, 1 mm for C-F.

the right and left OB of mutant mice (Fig. 2D,F, asterisks). Thus, *Arx* mutation severely impairs OB morphogenesis.

Reduced cell proliferation in *Arx*-deficient mice

To examine whether cell proliferation occurs normally in *Arx*-deficient mice, we performed a BrdU incorporation experiment at E14.5 when genesis of OB interneurons, but not projection neurons, takes place massively in the SVZ (Hinds, 1968). Mice were subjected to BrdU injection at E14.5 and killed after 1 hour. BrdU-positive cells in the SVZ from the OB to the ganglionic eminence were immunohistochemically stained with anti-BrdU antibody (Fig. 3A-F). The number of BrdU-positive cells in mutant OB (43±21) was significantly lower than that in wild-type OB (598±21) (n=3, P<0.01, t-test) (Fig. 3G). Also in the RMS and ganglionic eminence, the number of BrdU-positive cells in mutant mice (3,760±113) was reduced compared with that in wild-type mice (6,120±373) (n=3, P<0.05, t-test) (Fig. 3H). This result suggests that the *Arx* gene regulates the proliferation of OB interneuron progenitors.

Impaired entry of interneuron progenitors into OB in *Arx*-deficient mice

The detailed structure of the developing olfactory system was histologically analyzed on Nissl-stained parasagittal sections of wild-type (Fig. 4A,C,E) and *Arx*-deficient mice (Fig. 4B,D,F). At E12.5, *Arx*-deficient mice showed size reduction of the lateral and medial ganglionic eminence and enlargement of the brain ventricle, while the anterior telencephalon (OB anlagen) was indistinguishable between wild-type and mutant mice (Fig. 4A,B). At E16.5, the RMS became apparent as a densely packed cellular mass migrating from the ganglionic eminence to the OB

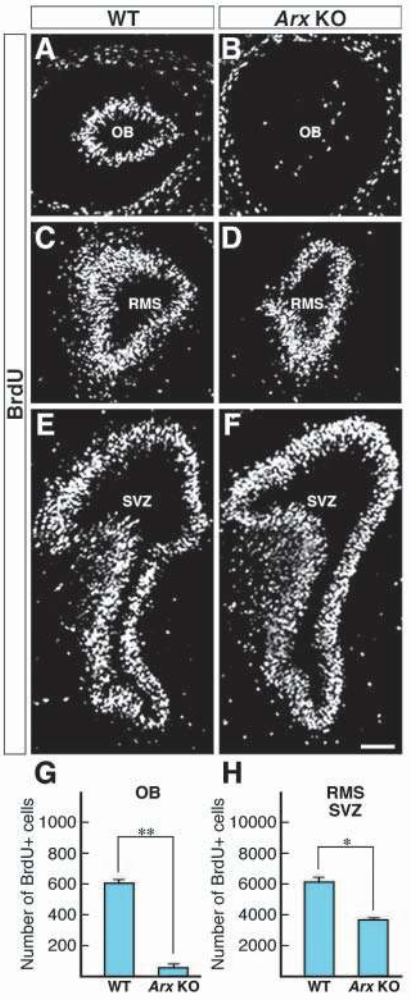

Fig. 3. Proliferation defect of OB interneuron progenitors in *Arx*-deficient mice. (A-F) Coronal sections of E14.5 olfactory bulb (OB; A,B), rostral migratory stream (RMS; C,D) and ganglionic eminence (E,F) of wild-type (A,C,E) and *Arx*-deficient (B,D,F) mice that incorporated BrdU for 1 hour were labeled with anti-BrdU antibody. BrdU-labeled cells were observed in the subventricular zone (SVZ) of wild-type and mutant mice. (G) Quantification of BrdU-positive cells in wild-type and mutant OB. Values are mean±s.e.m. (n=3, t-test, P<0.01, marked with double asterisks). (H) Quantification of BrdU-positive cells in wild-type and mutant RMS and SVZ. Values are mean±s.e.m. (n=3, t-test, P<0.05, marked with asterisk). Scale bar: 200 μm.

in wild-type mice (Fig. 4C). However, the RMS was greatly shortened in a rostrocaudal direction and thickened in mutant mice (Fig. 4D). A similar hypoplasia of the RMS was observed in mutant mice at P0 (Fig. 4E,F). In contrast, the structure of the OE was not affected at any developmental stages by the mutation of the *Arx* gene (Fig. 4B,D,F).

Since the RMS contains migrating OB interneuron progenitors, we examined expression of several differentiation markers for OB interneurons at P0. *Dlx2* and *Dlx5* genes are strongly expressed in OB interneuron progenitors within the RMS (Fig. 4G,I) and play important roles in their differentiation and migration (Bulfone et al., 1998; Levi et al., 2003; Long et al., 2003). Expression patterns of the two genes closely resembled that of Arx in wild-type mice (Fig. 4K). In *Arx*-

deficient mice, expression of both *Dlx2* and *Dlx5* was observed within the shortened and thickened RMS (Fig. 4H,J). A truncated and nonfunctional form of Arx protein can be detected with our antibodies in *Arx*-deficient mice. Expression of truncated Arx also displayed a similar pattern to *Dlx2* and *Dlx5* in the irregular RMS (Fig. 4L). Final differentiation of OB interneurons is associated with expression of the inhibitory neurotransmitter GABA. In wild-type OB, GABA immunoreactivity was detected in granule cells and periglomerular cells in the GCL and GL, respectively (Fig. 4M). In mutant mice, however, most of the GABA-positive neurons could not enter the OB and accumulated at the rostral end of the RMS (arrowheads) and ventrally apposing region (asterisk) (Fig. 4N).

To visualize the migration process of OB interneuron progenitors more clearly, we performed another BrdU labeling experiment. Pregnant mice received an injection of BrdU at E14.5 or E16.5 to label cells of different birth dates. In newborn mice (P0), BrdU-labeled cells were examined for their location along the migratory pathway of OB interneuron progenitors. In wild-type mice, numerous BrdU-labeled OB interneurons born at E14.5 were dispersed throughout GCL (Fig. S2A in the supplementary material), while younger interneurons and their progenitors born at E16.5 were more densely packed in the core region of the GCL and in the RMS (Fig. S2C in the supplementary material). In contrast, although the migration of interneuron progenitors in *Arx*-deficient mice was observed within the RMS, they stalled at the rostral tip of the RMS without entering into the OB (Fig. S2B,D in the supplementary material). These results suggest that *Arx* mutation affects the entry of interneuron progenitors into the OB, rather than the migration process within the RMS.

We asked whether the impaired entry of interneuron progenitors into the OB is cell-autonomous or non-cell-autonomous by analyzing *Arx* heterozygous female mice. Because the *Arx* gene is located on the X chromosome, *Arx* heterozygous female mice possess both Arx-expressing cells and *Arx*-deficient cells in a mosaic fashion. *Arx*-deficient cells can be detected by expression of β-galactosidase. The OB of *Arx* heterozygous female mice appeared normal with respect to the layer organization and olfactory axonal projection (data not shown). However, β-galactosidase-positive *Arx*-deficient interneuron progenitors were located only within the RMS and failed to enter the OB (Fig. 4O). This result indicates the impaired entry of *Arx*-deficient interneuron progenitors into the OB is cell-autonomous.

Loss of TH-positive interneurons in *Arx*-deficient mice

As shown above (Fig. 1K-R), TH is expressed by a subpopulation of the GABAergic periglomerular cells (Kosaka et al., 1995). We asked whether the *Arx* mutation influences development of TH(+) periglomerular cells. In wild-type mice, TH was expressed in Arx(+)/GABA(+) OB periglomerular cells and in Arx(–) midbrain dopaminergic neurons at E16.5 and P0 (Fig. 5A,C,E,G,I). In *Arx*-deficient mice, TH

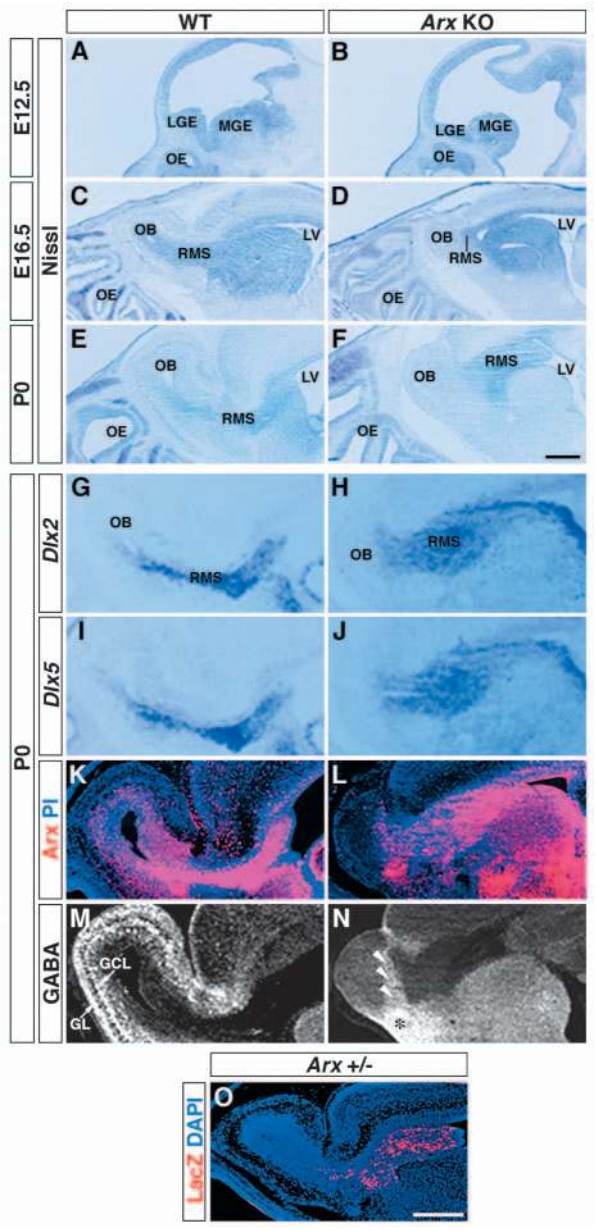

Fig. 4. Impaired entry of interneuron progenitors into the OB in *Arx*-deficient mice. Nissl-stained parasagittal sections of wild-type (A,C,E) and *Arx*-deficient (B,D,F) mice at E12.5 (A,B), E16.5 (C,D), and P0 (E,F). At E16.5 and P0, the mutant mouse had a smaller olfactory bulb (OB) and shortened rostral migratory stream (RMS) (D,F). (G-J) In situ hybridization analysis of *Dlx2* (G,H) and *Dlx5* (I,J) expression in wild-type (G,I) and mutant (H,J) mice at P0. (K,L) Parasagittal sections of wild-type (K) and mutant (L) mice at P0 were labeled with anti-Arx antibody (red) and counterstained with PI (blue). In the *Arx*-deficient mouse (L), the antibody can recognize a truncated non-functional Arx protein. (M,N) Immunohistochemical labeling of GABA in wild-type (M) and mutant (N) mice at P0. While GABA is expressed in periglomerular cells in glomerular layer (GL) and granule cells in the granule cell layer (GCL) in the wild-type mouse (M), GABA-expressing cells are observed at the rostral end (arrowheads) and ventrally apposing region (asterisk) of the RMS (N). (O) Parasagittal section of P0 *Arx* heterozygous female brain was labeled with anti-LacZ antibody (red) and counterstained with DAPI (blue). Because *Arx* is located on the X chromosome, the *Arx* heterozygous female mouse is mosaic for *Arx* deficiency. LacZ(+) *Arx*-deficient cells failed to enter the OB. LGE, lateral ganglionic eminence; LV, lateral ventricle; MGE, medial ganglionic eminence; OE, olfactory epithelium. Scale bars: in F, 400 μm for A-F; in O, 400 μm for G-O.

immunoreactivity was completely absent in OB and RMS (Fig. 5B,F,J), although GABA(+) cells were observed (Fig. 5H,J). On the other hand, TH(+) neurons were normally present in the substantia nigra of mutant mice (Fig. 5D). In addition, *Nurr1*, an orphan nuclear receptor expressed in TH(+) periglomerular cells in wild-type mice (Fig. 5K) (Backman et al., 1999; Liu and Baker, 1999), was not detected in *Arx*-deficient OB (Fig. 5L). These results indicate that *Arx* is required for the differentiation of TH(+) periglomerular cells.

Disorganization of the mitral cell layer in *Arx*-deficient mice

Development of OB projection neurons, mitral cells, was examined in *Arx*-deficient mice. Anti-Tbx21 staining clearly demarcated the MCL with a thickness of 2-4 mitral cells in wild-type mice at E16.5 and P0 (Fig. 6A,C,E). In contrast, mitral cells were scattered throughout the OB in mutant mice at E16.5 (Fig. 6B). Disorganized MCL was observed in mutant OB at P0, as a thicker and irregular contour (Fig. 6D,F), whereas the number of Tbx21(+) mitral cells in mutant mice (29,240±270, n=3) was almost equal to that in wild-type mice (29,680±650, n=3) at P0.

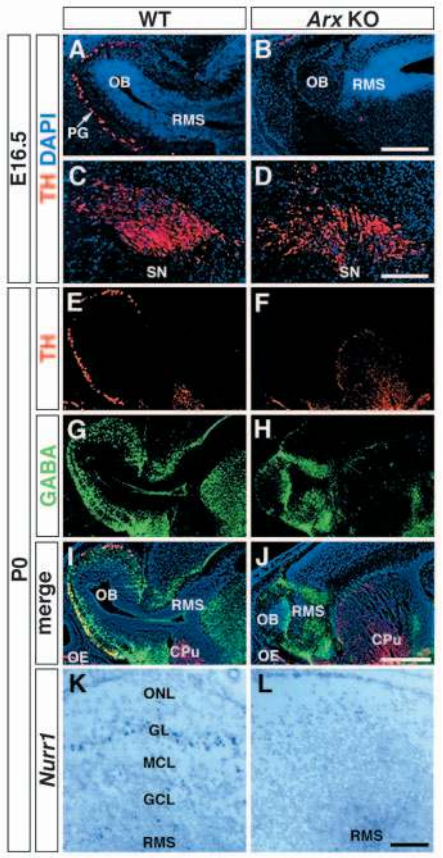

Fig. 5. Loss of TH(+) interneurons in the OB of *Arx*-deficient mice. (A-J) Parasagittal sections of E16.5 (A-D) and P0 (E-J) brains of wild-type (A,C,E,G,I) and *Arx*-deficient (B,D,F,H,J) mice were labeled with anti-TH antibody (red), anti-GABA antibody (green) and counterstained with DAPI (blue). In wild-type mice, TH immunoreactivity was observed in periglomerular cells (PG) in the olfactory bulb (OB) (A,E,I). However, no TH(+) cells were detected in the OB or the rostral migratory stream (RMS) of mutant mice (B,F,J). In contrast, differentiation of TH(+) cells in the substantia nigra (SN) was not affected (D). TH signals in the caudate putamen (CPu) are derived from axon terminals of dopaminergic neurons in the SN (E,F,I,J). (K,L) In situ hybridization analysis of *Nurr1* expression on OB coronal sections of P0 wild-type (K) and mutant (L) mice. In the wild-type mouse (K), *Nurr1*(+) cells were observed in the glomerular layer (GL) and granule cell layer (GCL), whereas no *Nurr1*-positive cells were observed in mutant OB (L). MCL, mitral cell layer; OE, olfactory epithelium; ONL, olfactory nerve layer. Scale bars: in B, 400 μm for A,B; in D, 200 μm for C,D; in J, 800 μm for E-J; in L, 100 μm for K,L.

Mitral cells send their axons to the olfactory cortex through the lateral olfactory tract (LOT). Structure of the LOT was analyzed by immunostaining of L1, a cell adhesion molecule abundantly expressed in all mitral cell axons (Inaki et al., 2004). The LOT of *Arx*-deficient mice was indistinguishable from that of wild-type mice (Fig. 6G,H). Thus, in spite of the disorganization of the MCL in the OB, mitral cells projected their axons normally to form the LOT in *Arx*-deficient mice.

The morphology of mitral cells was examined by triple fluorescent labeling with three antibodies: anti-Thy-1 (Fig. 6I,J,O,P, whole dendrite labeling) (Xue et al., 1990), anti-Reelin (Fig. 6K,L,O,P, proximal dendrite labeling) (Long et al., 2003), and anti-Tbx21 (Fig. 6M-P, cell body labeling). In wild-type mice, all mitral cells projected their dendrites regularly and consistently toward the apical direction (Fig. 6I,K,M,O). In contrast, the orientation of proximal dendrites of mitral cells was variable in *Arx*-deficient mice (Fig. 6L,P), while distal dendrites normally located in the apical portion of the OB (Fig. 6J,P). In addition, Thy-1 immunoreactivity in the proximal dendrites was absent in mutant mice (Fig. 6J,P). These results suggest that *Arx* mutation causes disorganization of the MCL.

Abnormal projection of olfactory axons in *Arx*-deficient mice

We next asked whether the disorganized OB structure might affect axonal projection of the olfactory sensory neurons from the OE to the OB. At E12.5, olfactory pioneer axons first reached the OB anlagen at the anterior tip of the telencephalon in both wild-type and *Arx*-deficient mice (Fig. 7A,B). At E16.5, no difference was observed with respect to the gross morphology of the OE and the differentiation of OMP-positive sensory neurons between wild-type and mutant mice (Fig. 7C-F). However, there was a clear difference in the trajectory of olfactory axons at E16.5. In wild-type mice, all olfactory axons reached and surrounded OB to form ONL (Fig. 7G). In contrast, most of the olfactory axons in mutant mice failed to reach the OB and formed a large tangled sphere between the OE and OB (Fig. 7H, asterisk), a structure called the 'fibrocellular mass' (FCM) first identified in naturally occurring mutant mouse *extratoes* (*Xt*/*Xt*) (St John et al., 2003). Only a small fraction of olfactory axons was in direct contact with the surface of the OB (Fig. 7H, arrowheads).

At P0, the layer organization of the OB was clearly visible in wild-type mice that could be defined by differential expression of several marker molecules: NCAM (olfactory axons) (Fig. 8A,G,I), Tbx21 (mitral cells) (Fig. 8C,G), GABA (periglomerular cells and granule cells) (Fig. 8E,G), neuropeptide Y (olfactory ensheathing glia in the inner portion of the ONL) (Au et al., 2002) (Fig. 8K), S100 (olfactory ensheathing glia in the outer portion of ONL) (Au et al., 2002) (Fig. 8M), and GLAST (radial glia) (Fig. 8O). In contrast, the layer structure was severely distorted in mutant OB (Fig.

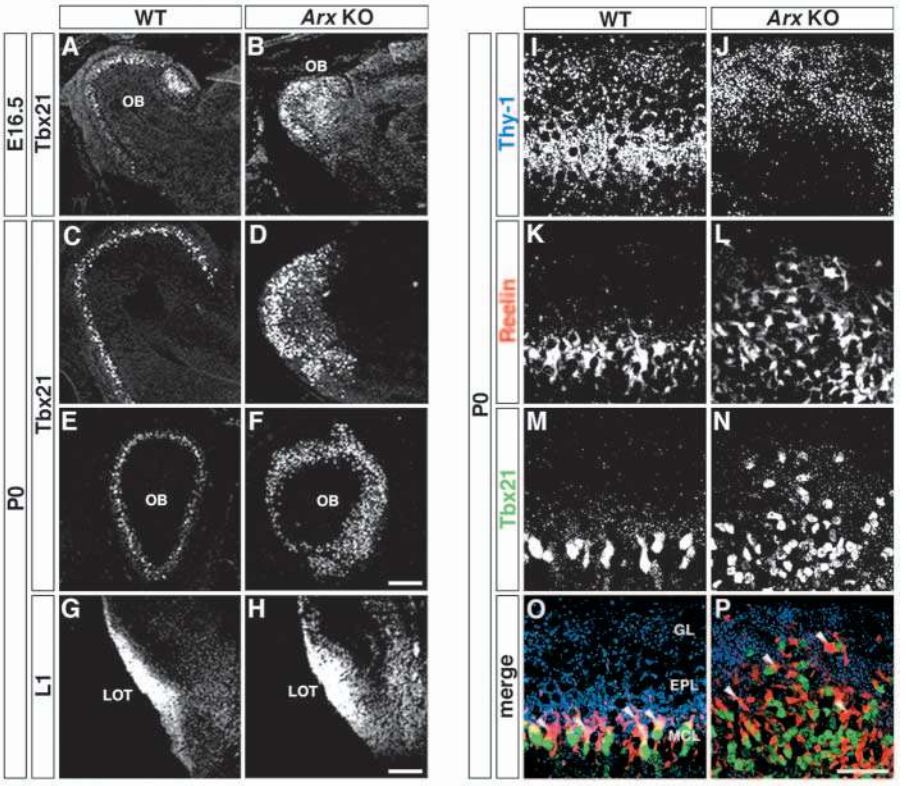

Fig. 6. Abnormal distribution of mitral cells and their dendrites in *Arx*-deficient mice. (A-F) Immunohistochemical analysis of Tbx21 expression in the olfactory bulb (OB) parasagittal sections (A-D) and coronal sections (E,F). In *Arx*-deficient mice at E16.5 (B) and P0 (D,F), mitral cells were found widely scattered in the OB, compared to wild-type (A,C,E). In a coronal section of the mutant OB (F), the mitral cell layer (MCL) showed an irregular contour: the MCL in the medial side of the OB (the right side in F) was thicker than in the lateral side (the left side in F). (G,H) Immunohistochemical analysis of L1 expression in the lateral olfactory tract (LOT) in coronal sections of P0 wild-type (G) and mutant (H) mice. LOT formation was normal in both mice. (I-P) Immunohistochemical analysis of Thy-1 (blue: whole dendrites of mitral cells) (I,J,O,P), reelin (red: proximal dendrites of mitral cells) (K,L,O,P), and Tbx21 (green: somata of mitral cells) (M,N,O,P) expression. In wild-type mice, mitral cell dendrites labeled with Thy-1 and reelin extended in a radial direction (I,K, arrowheads in O). In mutant mice, the orientation of proximal dendrites was variable (L, arrowheads in P), but the distal dendrites tend to reach the apical region of the OB (J,P). Thy-1 immunoreactivity in proximal dendrites in mutant mice disappeared (J,P). EPL, external plexiform layer; GL, glomerular layer. Scale bars: in F, 200 μm for A-F; in H, 100 μm for G,H; in P, 50 μm for I-P.

8B,D,F,H,L,N,P). At only the anterodorsomedial surface of disorganized OB, ONL was present where neuropeptide Y(+) and S100(+) ensheathing cells were observed normally in the inner and outer portions, respectively (Fig. 8L,N). In addition, the apically projecting fibers of GLAST(+) radial glia were found only beneath the ONL at the anterodorsomedial surface of the OB, where the innervation of olfactory axons occurred (Fig. 8P, arrowheads). However, protoglomeruli observed in wild-type OB (Fig. 8I, arrowheads) were not detected in mutant OB (Fig. 8J). The FCM was situated in close apposition to the anteromedial surface of the OB in mutant mice (Fig. 8B,H,L,N,P, asterisks) and contained S100(+) olfactory ensheathing glia as well as olfactory axons (Fig. 8N, asterisk).

Segregation of different subsets of olfactory axons in the FCM

Finally, we investigated whether the segregation of olfactory axons is retained in the FCM by analyzing expression patterns of three cell recognition molecules: OCAM, neuropilin-1, and neuropilin-2. The OE is divided into four circumscribed zones that are defined by spatially non-overlapping expression of odorant receptor genes (Ressler et al., 1993; Vassar et al., 1993). Olfactory sensory neurons in a given OE zone project their axons to glomeruli in a corresponding zone of the OB (zone-to-zone projection) (Mori et al., 2000). OCAM is a cell adhesion molecule specifically localized to the olfactory axons of three ventrolateral zones of the OE (zones II, III, IV), but not to the most dorsomedial zone (zone I), while NCAM is expressed in all olfactory axons (Yoshihara et al., 1997; Mori et al., 2000; Nagao et al., 2000). In wild-type mice, OCAM(+) zone II-IV axons (yellow) and OCAM(–) zone I axons (red) innervated topographically segregated zones on the surface of OB (Fig. 8Q). In *Arx*-deficient mice, although most of the olfactory axons did not reach the OB, a clear segregation of OCAM(–) zone I axons and OCAM(+) zone II-IV axons was apparent in the FCM (Fig. 8R, asterisk).

Neuropilin-1 and -2 are cell surface receptors for chemorepellents of semaphorin family molecules (Raper, 2000). Neuropilin-1 is expressed in a subset of olfactory axons that terminate in two unique symmetrical domains in the medial and lateral hemispheres of the OB (two yellow regions in Fig. 8S) (Nagao et al., 2000). In the FCM of *Arx*-deficient mice, a segregation of neuropilin-1(+) and (–) axons was clearly observed with a sharp boundary (Fig. 8T, asterisk). Manners of segregation were different between OCAM and neuropilin-1 (Fig. 8R,T, asterisks). Neuropilin-2 is expressed in a small subset of olfactory axons that terminate in the most anteromedial region and most posterior region of the OB (yellow regions in Fig. 8U) (Norlin et al., 2001). In mutant mice, neuropilin-2(+) axons were observed in small regions at the edge of the FCM, while neuropilin-2(–) axons occupied the central portion of the FCM (Fig. 8V, asterisk). Thus, olfactory axons showed clear segregation that can be defined by differential expression of the cell recognition molecules in the FCM. This result suggests that the segregation of olfactory axons is independent of the direct contact with target OB.

As mentioned above (Fig. 8H), a small subset of olfactory axons could reach the anteromedial surface of the OB in *Arx*-deficient mice. These axons were positive for OCAM and neuropilin-2, but negative for neuropilin-1 (arrowheads in Fig.

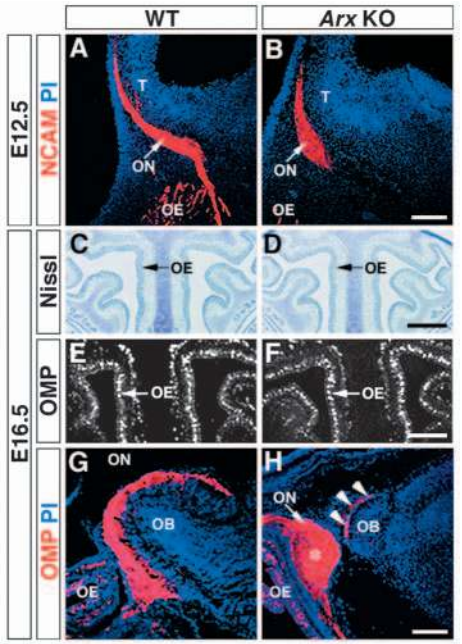

Fig. 7. Abnormal projection of olfactory axons in *Arx*-deficient mice. (A,B) Immunofluorescence labeling of NCAM (red: olfactory axons) and PI staining (blue: nucleus) on parasagittal sections of E12.5 wild-type (A) and *Arx*-deficient (B) mice. In both mice, pioneer olfactory axons reached the anterior tip of the telencephalon (T). (C,D) Coronal sections of Nissl-stained olfactory epithelium (OE) of E16.5 wild-type (C) and mutant (D) mice. (E,F) Immunohistochemical analysis of olfactory marker protein (OMP) expression in mature olfactory sensory neurons in the OE of E16.5 wild-type (E) and mutant (F) mice. (G,H) Immunofluorescence labeling of OMP (red: olfactory axons) and PI staining (blue: nucleus) on parasagittal sections of the olfactory bulb (OB) from E16.5 wild-type (G) and mutant (H) mice. In mutant mice, a small subpopulation of olfactory nerve (ON) kept contact with the OB (arrowheads in H). However, most of the ON did not reach the OB and terminated in an unusual axon-tangled structure, the FCM, in front of the OB (asterisk in H). Scale bars: in B, 100 μm for A,B; in D, 400 μm for C,D; in F, 600 μm in E,F; in H, 200 μm for G,H.

8R,T,V). In wild-type OB, the anteromedial cluster of OCAM(+)/neuropilin-1(–)/neuropilin-2(+) glomeruli was called 'a tongue-shaped area' (arrowheads in Fig. 8Q,S,U) (Nagao et al., 2000). From the topographical location and molecular expression, the OB region innervated by these olfactory axons in *Arx*-deficient mice may correspond to the tongue-shaped area in the wild-type mice.

Discussion

Abnormalities in the olfactory system caused by the *Arx* mutation

Fig. 9 depicts a summarized diagram illustrating the OB structure of wild-type and *Arx*-deficient mice at P0. We found several abnormalities in cellular organization, differentiation, and axonal projection in the developing olfactory system of mutant mice.

OB interneurons (granule cells and periglomerular cells) are derived from progenitors in the lateral ganglionic eminence that migrate rostrally through the RMS towards the OB (Luskin, 1998; Wichterle et al., 2001). Arx is strongly expressed in these interneurons and their progenitors in the OB and RMS. In *Arx*-deficient mice, we found that their proliferation and migration into the OB were severely impaired and that they accumulated at the entrance point of the OB. A similar phenotype was also reported in respect of the interneuron proliferation and migration from the medial ganglionic eminence to the neocortex of *Arx*-deficient mice (Kitamura et al., 2002). Although the birth place, migratory route, and final destination are different between the neocortex and OB interneurons, there may be a common mechanism underlying the directed neuronal migration in both systems, and Arx may play an important role in this process possibly by controlling the expression of unknown downstream genes in a cell-autonomous way. Although we surveyed the expression of several candidate molecules that may regulate OB interneuron migration from the SVZ to the OB through the RMS, including PSA-NCAM (Tomasiewicz et al., 1993; Cremer et al., 1994), Robo/Slit (Nguyen-Ba-Charvet et al., 2004), ephrin/Eph (Conover et al., 2000), integrin, and DCC (Murase and Horwitx, 2002), they were expressed in *Arx*-deficient mice in patterns similar to wild-type mice (Fig. S3A-X in the supplementary material). In addition, the primordium of RMS glial tunnel consisting of radial glia (Hartfuss et al., 2001) was observed from the striatal SVZ to the OB in both wild-type and *Arx*-deficient mice (Fig. S3Y,Z in the supplementary material). cDNA microarray analysis is currently ongoing in our laboratory to search for downstream genes of Arx, that play crucial roles in the entry of interneurons into the OB.

Although the expression of GABA was observed in *Arx*-deficient mice, a TH(+) subpopulation of GABAergic interneurons was completely absent in the OB. Moreover, the OB of mutant mice lacked expression of *Nurr1*, a putative transcription factor regulating differentiation of TH(+) OB interneurons (Backman et al., 1999; Liu and Baker, 1999). These results indicate that *Arx* mutation affects differentiation of a specific type of OB interneurons. A plausible explanation for this phenotype would be that the *Arx* gene may be located upstream of *Nurr1* and *TH* genes in a genetic cascade for the differentiation. However, we cannot exclude a possibility that the progenitors of TH(+) OB interneurons may not be exposed to appropriate differentiation signals produced in the OB due to the impaired entry into the OB.

Although Arx is not expressed in mitral cells, disorganization of the MCL was observed as a thicker and irregular contour. Since massive addition of interneurons from the RMS results in the expansion of the OB at late embryonic stages, we assume that the disorganization of the MCL in *Arx*-deficient mice is caused by the decrease of the GCL resulting from the impaired entry of interneurons into the OB. Another possibility is that Arx may be expressed in progenitors of OB projection neurons. Recently, it was reported that radial glia are progenitors for the majority of neurons in the brain (Anthony et al., 2004). If it is also the case for OB projection neurons, the abnormal layering of OB projection neurons may be attributable to a cell-autonomous defect caused by *Arx* mutation in radial glia. Alternatively, putative signal(s) may be missing in *Arx*-deficient mice, which is produced by OB interneurons, radial glia, or olfactory sensory neurons and directs normal layering of OB projection neurons.

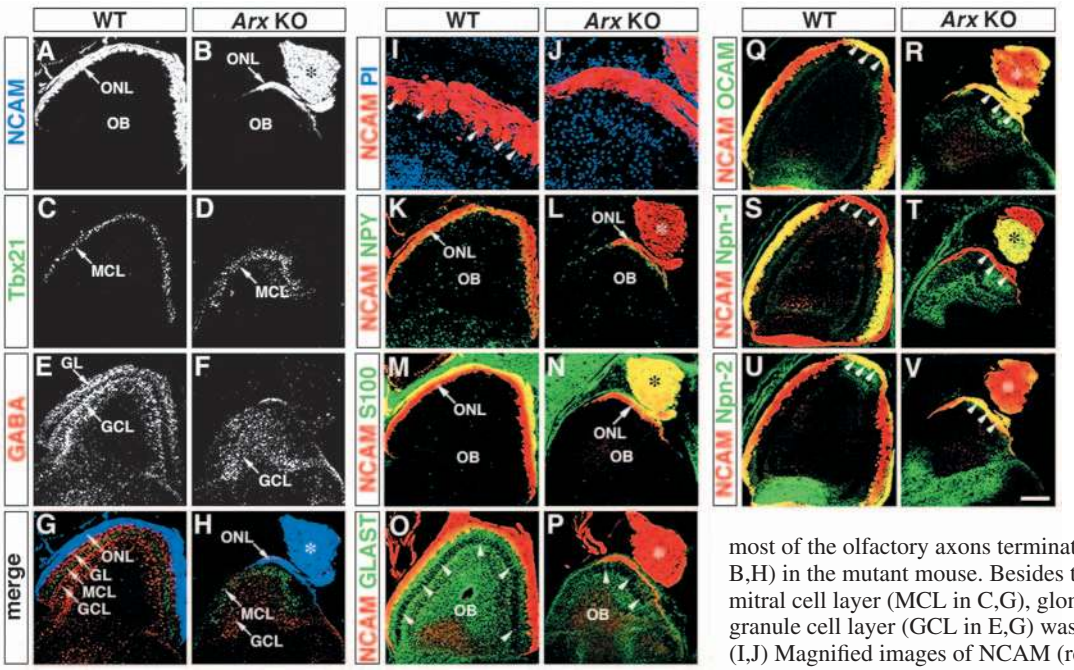

Fig. 8. Disorganization of OB layer structure in *Arx*-deficient mice. (A-H) Immunohistochemical analysis of NCAM (blue: olfactory axons) (A,B,G,H), Tbx21 (green: mitral cells) (C,D,G,H), and GABA (red: interneurons) (E,F,G,H) expression on horizontal sections of olfactory bulb (OB) from wild-type (A,C,E,G) and *Arx*-deicient (B,D,F,H) mice at P0. In the wild-type mouse, the olfactory nerve layer (ONL) surrounded the whole surface of the OB (A,G). In contrast, the ONL was present only in the rostromedial side (right side in B) of the OB and most of the olfactory axons terminated in the FCM (asterisks in B,H) in the mutant mouse. Besides the ONL, the formation of the mitral cell layer (MCL in C,G), glomerular layer (GL in E,G), and granule cell layer (GCL in E,G) was affected in mutant OB (D,F,H). (I,J) Magnified images of NCAM (red) and DAPI (blue) labeling on OB horizontal sections of P0 wild-type (I) and mutant (J) mice. Protoglomeruli structures (arrowheads in I) were only observed in wild-type OB. (K,L) Immunohistochemical analysis of NCAM (red: olfactory axons) and neuropeptide Y (NPY) (green: olfactory ensheathing glia in the inner ONL) expression on horizontal sections of P0 wild-type (K) and mutant (L) mice. NPY immunoreactivity was observed in the inner portion of the ONL in both wild-type and mutant OB. (M,N) Immunohistochemical analysis of NCAM (red: olfactory axons) and S100 (green: olfactory ensheathing glia in the outer ONL) expression in P0 wild-type (M) and mutant (N) mice. S100 immunoreactivity was observed in the outer portion of the ONL in both wild-type and mutant OB and in the FCM (asterisk in N) of mutant mouse. (O,P) Immunohistochemical analysis of NCAM (red: olfactory axons) and GLAST (green: radial glia) expression in P0 wild-type (O) and mutant (P) mice. GLAST(+) radial processes were observed throughout the OB of the wild-type mouse (arrowheads in O). In contrast, radial processes were only found in the rostromedial region of mutant OB (arrowheads in P) where the innervation of olfactory axons occurred. (Q-V) Immunohistochemical analysis of expression patterns of cell recognition molecules on horizontal sections of P0 wild-type (Q,S,U) and *Arx*-deficient (R,T,V) mice. (Q,R) NCAM (red) and OCAM (green). (S,T) NCAM (red) and neuropilin-1 (Npn-1) (green). (U,V) NCAM (red) and neuropilin-2 (Npn-2) (green). Arrowheads in (Q,S,U) indicate the OCAM(+)/Npn-1(–)/Npn-2(+) tongue-shaped area in the wild-type mouse (Nagao et al., 2000). Arrowheads in R,T,V indicate a subpopulation of olfactory axons reaching the OB in the mutant mouse. Asterisks in R,T,V: FCM. Scale bar: in V, 200 μm for A-H and K-V; 50 μm for I,J.

A non-cell-autonomous defect was seen in the projection pattern of olfactory sensory neurons. In *Arx*-deficient mice, most of the olfactory axons failed to reach the OB and terminated in a tangled structure, the FCM, in front of the OB (discussed below).

Transcription factors regulating development of OB interneurons

Three members of the Dlx transcription factor family (*Dlx-1, -2, -5*) have been proposed to play crucial roles in development of the olfactory system. They are expressed in the OB interneurons and their progenitors with consecutively differential but overlapping patterns (Bulfone et al., 1998; Levi et al., 2003; Long et al., 2003). The *Dlx-1* and *Dlx-2* double knockout mice show the most severe defects in the proliferation and migration of the OB interneurons: they are completely absent (Bulfone et al., 1998). In contrast, the phenotypes of *Dlx-5*-deficient mice are milder and, to some extent, similar to those of the *Arx*-deficient mice, including (a) size reduction of the OB, (b) impaired migration of OB interneurons, (c) the disorganization of the MCL, and (d) impaired axonal projection of olfactory sensory neurons forming the FCM. Unlike *Arx*, however, *Dlx-5* is also expressed in the olfactory sensory neurons and its mutation causes a drastically reduced proliferation, raising a possibility that some of the above-mentiond phenotypes may be attributable to abnormality in the sensory neurons (Levi et al., 2003; Long et al., 2003). Because we detected the expression of *Dlx-2* and *Dlx-5* in the *Arx*-deficient mice, the *Arx* gene may play roles in a genetic cascade different from the *Dlx* cascade, or downstream of *Dlx* genes. Analysis of *Arx* expression in the *Dlx-5*-deficient mice would provide an answer to this issue.

Bidirectional interactions between OE and OB during development

A possibility of mutual influences between the OE and OB on inductive and developmental processes has been proposed and extensively studied (for a review, see López-Mascaraque and de Castro, 2002). In *Xenopus*, the surgical ablation of olfactory placode results in loss or hypoplasia of the OB (Stout and Graziadei, 1980; Graziadei and Monti-Graziadei, 1992; Byrd and Burd, 1993). In rats, the arrival of pioneer olfactory axons regulates the cell cycle kinetics and the rate of differentiation of neuronal progenitors to induce the formation of the OB (Gong and Shipley, 1995). In mice deficient of the olfactory cyclic nucleotide-gated channel specifically expressed in olfactory sensory neurons, the OB is smaller than in wild-type

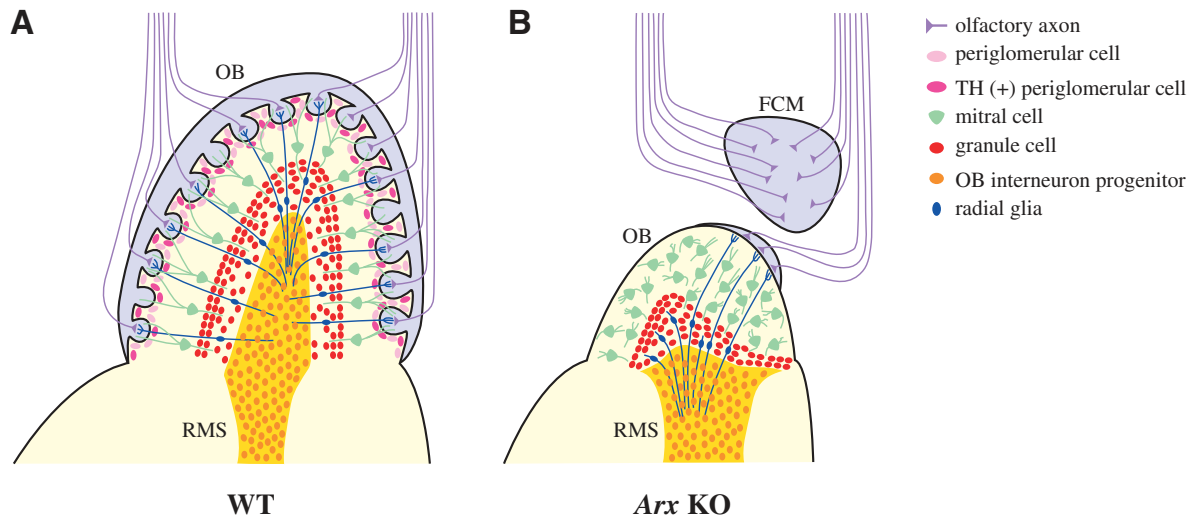

Fig. 9. A schematic representation of OB structures in wild-type and *Arx*-deficient mice at P0. Diagrams show horizontal sections of the olfactory bulb (OB) in wild-type (A) and *Arx*-deficient mice (B). Anterior is to the top and lateral is to the left. Mutant mice showed the impaired entry of interneuron progenitors (orange) into the OB, the loss of TH(+) periglomerular cells (dark pink), and the disorganization of OB layer structure. The innervation of olfactory axons (purple) and the apical projection of radial glial fibers (blue) were observed only at the rostromedial side of OB in mutant mice. The olfactory axons that failed to reach mutant OB formed the fibrocellular mass (FCM) in front of the OB. RMS, rostral migratory stream.

mice (Lin et al., 2000). These studies suggest that the OE somehow influences the development of the OB.

Then, how about the influence in an opposite direction: from the OB to the OE? This possibility was studied mainly using the *Gli3* mutant mice, *extratoes*. The OB is completely absent in *Gli3*-deficient mice and OB projection neurons distributed sparsely on the surface of rostrolateral forebrain undergo apoptosis (Hui and Joyner, 1993; St John et al., 2003). On the other hand, OE development proceeds normally in respect of its gross morphology and expression of signal transduction molecules including odorant receptors (Sullivan et al., 1995). However, olfactory axons do not reach the telencephalon and instead terminate in the abnormal structure called the FCM (St John et al., 2003). Thus, the OB appears not to influence the cellular proliferation and differentiation of the OE, but may have an instructive role in guidance of the olfactory axons. In *Arx*-deficient mice, only a small population of olfactory axons made contact with the OB, but most of them failed to reach the OB and terminated in the FCM. Because Arx is not expressed in the olfactory sensory neurons, we assume that Arx regulates the expression of putative instructive signal(s) produced in the OB for proper innervation of olfactory axons. Although the identity of such signal(s) is unknown yet, we speculate that it may be produced in OB radial glia for the following reasons. (1) Olfactory axons innervate the OB normally in *Dlx1/Dlx2* double mutant mice that lack OB interneurons (Bulfone et al., 1998). Therefore, the involvement of OB interneurons is excluded. (2) Olfactory axons innervate the OB normally in *Tbr1* mutant mice that lack OB projection neurons (Bulfone et al., 1998), eliminating the involvement of OB projection neurons. (3) *Arx* is expressed only in radial glia and interneurons of the OB, but not in other types of cells in the olfactory system. Its mutation causes the failure of olfactory axon projection. (4) Development of OB radial glia closely correlates with the projection of olfactory axons and formation of glomeruli (Bailey et al., 1999; Puche and Shipley, 2001). Further investigation is necessary to clarify the identity and origin of this putative instructive signal(s) in the developing olfactory system.

In *Arx*-deficient mice at P0, a small subset of olfactory axons kept contact with the rostromedial region of the OB and were positive for OCAM and neuropilin-2, but negative for neuropilin-1, reminiscent of the tongue-shaped area of the OB in wild-type mice (Nagao et al., 2000). Our analysis revealed that the pioneer olfactory axons could reach the anterior tip of the telencephalon in both wild-type and *Arx*-deficient mice at E12.5 (Fig. 7A,B). These earliest growing axons were also positive for OCAM and neuropilin-2, but negative for neuropilin-1 (data not shown). Thus, a subset of olfactory axons reaching mutant OB at E16.5 (Fig. 7H) and P0 (Fig. 8) appears to be a remnant of the pioneer axons. If so, a target region innervated by pioneer axons becomes the future 'tongue-shaped area' in the OB. Thus, *Arx*-deficient mice provide an important clue for a likely relationship between the innervation of pioneer olfactory axons at early developmental stages and the formation of the 'tongue-shaped area' in the glomerular map of adult OB. Furthermore, based on this assumption, the olfactory axons that fail to contact mutant OB may be derived from the 'follower' olfactory axons, but not from the 'pioneer' axons. We speculate that Arx regulates the expression of putative instructive signal(s) produced in the OB for proper innervation of the 'follower' axons, but not the 'pioneer' axons.

Interestingly, olfactory axons in the FCM of *Arx*-deficient mice are clearly segregated with respect to the expression of cell recognition molecules (Fig. 8R,T,V). This result indicates that the segregation of different subsets of olfactory axons takes place even without direct contact with the OB. This notion is supported by a previous report describing that, in *Gli3* mutant mice, the olfactory axons originating from the sensory neurons expressing an odorant receptor P2 are able to sort out from other axons and converge to specific loci in the FCM (St

John et al., 2003). This phenomenon may be achieved by using intrinsic machineries equipped in the olfactory axons. Alternatively, there may be an influence from other cells in the environment such as the olfactory ensheathing glia that have been reported to play an important role in olfactory axon sorting in developing moth *Manduca sexta* (Oland et al., 1998; Higgins et al., 2002).

We thank F. L. Margolis (University of Maryland), F. Murakami (Osaka University), M. Ogawa (RIKEN BSI), T. Seki (Juntendo University), and A. Tamada (RIKEN BSI) for antibodies, M. Yokoyama, K. Nakamura, and R. Suzuki-Migishima (Mitsubishi Kagaku Insitute of Life Sciences) for support in production and maintenance of *Arx*-deficient mice, N. Hirotani, M. Kumai and members of the Research Resource Center (RIKEN BSI) for technical support in production of anti-Tbx21 antibody, and members of the Yoshihara lab for helpful discussions. This work was supported by research grants from RIKEN BSI.

Supplementary material

Supplementary material for this article is available at
http://dev.biologists.org/cgi/content/full/132/4/751/DC1

References

Anthony, T. E., Klein, C., Fishell, G. and Heintz, N. (2004). Radial glia serve as neuronal progenitors in all regions of the central nervous system. *Neuron* **41**, 881-890.

Au, W. W., Treloar, H. B. and Greer, C. A. (2002). Sublaminar organization of the mouse olfactory bulb nerve layer. *J. Comp. Neurol.* **446**, 68-80.

Backman, C., Perlmann, T., Wallen, A., Hoffer, B. J. and Morales, M. (1999). A selective group of dopaminergic neurons express Nurr1 in the adult mouse brain. *Brain Res.* **851**, 125-132.

Bailey, M. S., Puche, A. C. and Shipley, M. T. (1999). Development of the olfactory bulb: evidence for glia-neuron interactions in glomerular formation. *J. Comp. Neurol.* **415**, 423-448.

Bienvenu, T., Poirier, K., Friocourt, G., Bahi, N., Beaumont, D., Fauchereau, F., Ben Jeema, L., Zemni, R., Vinet, M. C., Francis, F. et al. (2002). ARX, a novel Prd-class-homeobox gene highly expressed in the telencephalon, is mutated in X-linked mental retardation. *Hum. Mol. Genet.* **11**, 981-991.

Bulfone, A., Wang, F., Hevner, R., Anderson, S., Cutforth, T., Chen, S., Meneses, J., Pedersen, R., Axel, R. and Rubenstein, J. L. (1998). An olfactory sensory map develops in the absence of normal projection neurons or GABAergic interneurons. *Neuron* **21**, 1273-1282.

Byrd, C. A. and Burd, G. D. (1993). The quantitative relationship between olfactory axons and mitral/tufted cells in developing *Xenopus* with partially deafferented olfactory bulbs. *J. Neurobiol.* **24**, 1229-1242.

Collombat, P., Mansouri, A., Hecksher-Sorensen, J., Serup, P., Krull, J., Gradwohl, G. and Gruss, P. (2003). Opposing actions of Arx and Pax4 in endocrine pancreas development. *Genes Dev.* **17**, 2591-2603.

Conover, J. C., Doetsch, F., Garcia-Verdugo, J. M., Gale, N. W., Yancopoulos, G. D. and Alvarez-Buylla, A. (2000). Disruption of Eph/ephrin signaling affects migration and proliferation in the adult subventricular zone. *Nat. Neurosci.* **3**, 1091-1097.

Cremer, H., Lange, R., Christoph, A., Plomann, M., Vopper, G., Roes, J., Brown, R., Baldwin, S., Kraemer, P. and Scheff, S. (1994). Inactivation of the N-CAM gene in mice results in size reduction of the olfactory bulb and deficits in spatial learning. *Nature* **367**, 455-459.

Faedo, A., Ficara, F., Ghiani, M., Aiuti, A., Rubenstein, J. L. and Bulfone, A. (2002). Developmental expression of the T-box transcription factor T-bet/Tbx21 during mouse embryogenesis. *Mech. Dev.* **116**, 157-160.

Gong, Q. and Shipley, M. T. (1995). Evidence that pioneer olfactory axons regulate telencephalon cell cycle kinetics to induce the formation of the olfactory bulb. *Neuron* **14**, 91-101.

Graziadei, P. P. and Monti-Graziadei, A. G. (1992). The influence of the olfactory placode on the development of the telencephalon in *Xenopus laevis*. *Neuroscience* **46**, 617-629.

Hartfuss, E., Galli, R., Heins, N. and Gotz, M. (2001). Characterization of CNS precursor subtypes and radial glia. *Dev. Biol.* **229**, 15-30.

Higgins, M. R., Gibson, N. J., Eckholdt, P. A., Nighorn, A., Copenhaver, P. F., Nardi, J. and Tolbert, L. P. (2002). Different isoforms of fasciclin II are expressed by a subset of developing olfactory receptor neurons and by olfactory-nerve glial cells during formation of glomeruli in the moth Manduca sexta. *Dev. Biol.* **244**, 134-154.

Hinds, J. W. (1968). Autoradiographic study of histogenesis in the mouse olfactory bulb. I. Time of origin of neurons and neuroglia. *J. Comp. Neurol.* **134**, 287-304.

Hui, C. C. and Joyner, A. L. (1993). A mouse model of greig cephalopolysyndactyly syndrome: the extra-toesJ mutation contains an intragenic deletion of the Gli3 gene. *Nat. Genet.* **3**, 241-246.

Inaki, K., Nishimura, S., Nakashiba, T., Itohara, S. and Yoshihara, Y. (2004). Laminar organization of the developing lateral olfactory tract revealed by differential expression of cell recognition molecules. *J. Comp. Neurol.* **479**, 243-256.

Keller, A. and Margolis, F. L. (1975). Immunological studies of the rat olfactory marker protein. *J. Neurochem.* **24**, 1101-1106.

Kitamura, K., Yanazawa, M., Sugiyama, N., Miura, H., Iizuka-Kogo, A., Kusaka, M., Omichi, K., Suzuki, R., Kato-Fukui, Y., Kamiirisa, K. et al. (2002). Mutation of *ARX* causes abnormal development of forebrain and testes in mice and X-linked lissencephaly with abnormal genitalia in humans. *Nat. Genet.* **32**, 359-369.

Kosaka, K., Aika, Y., Toida, K., Heizmann, C. W., Hunziker, W., Jacobowitz, D. M., Nagatsu, I., Streit, P., Visser, T. J. and Kosaka, T. (1995). Chemically defined neuron groups and their subpopulations in the glomerular layer of the rat main olfactory bulb. *Neurosci. Res.* **23**, 73-88.

Levi, G., Puche, A. C., Mantero, S., Barbieri, O., Trombino, S., Paleari, L., Egeo, A. and Merlo, G. R. (2003). The *Dlx5* homeodomain gene is essential for olfactory development and connectivity in the mouse. *Mol. Cell. Neurosci.* **22**, 530-543.

Lin, D. M., Wang, F., Lowe, G., Gold, G. H., Axel, R., Ngai, J. and Brunet, L. (2000). Formation of precise connections in the olfactory bulb occurs in the absence of odorant-evoked neuronal activity. *Neuron* **26**, 69-80.

Liu, N. and Baker, H. (1999). Activity-dependent Nurr1 and NGFI-B gene expression in adult mouse olfactory bulb. *Neuroreport* **17**, 747-751.

Long, J. E., Garel, S., Depew, M. J., Tobet, S. and Rubenstein, J. L. (2003). *DLX5* regulates development of peripheral and central components of the olfactory system. *J. Neurosci.* **23**, 568-578.

López-Mascaraque, L. and de Castro, F. (2002). The olfactory bulb as an independent developmental domain. *Cell Death Differ.* **9**, 1279-1286.

Luskin, M. B. (1998). Neuroblasts of the postnatal mammalian forebrain: their phenotype and fate. *J. Neurobiol.* **36**, 221-233.

Miura, H., Yanazawa, M., Kato, K. and Kitamura, K. (1997). Expression of a novel aristaless related homeobox gene 'Arx' in the vertebrate telencephalon, diencephalon and floor plate. *Mech. Dev.* **65**, 99-109.

Mori, K., Nagao, H. and Yoshihara, Y. (1999). The olfactory bulb: coding and processing of odor molecule information. *Science* **286**, 711-715.

Mori, K., von Campenhausen, H. and Yoshihara, Y. (2000). Zonal organization of the mammalian main and accessory olfactory systems. *Philos. Trans. R. Soc. Lond. Ser. B.* **355**, 1801-1812.

Murase, S. and Horwitz, A. F. (2002). Deleted in colorectal carcinoma and differentially expressed integrins mediate the directional migration of neural precursors in the rostral migratory stream. *J. Neurosci.* **22**, 3568-3579.

Nagao, H., Yoshihara, Y., Mitsui, S., Fujisawa, H. and Mori, K. (2000). Two mirror-image sensory maps with domain organization in the mouse main olfactory bulb. *Neuroreport* **11**, 3023-3027.

Nguyen-Ba-Charvet, K. T., Picard-Riera, N., Tessier-Lavigne, M., Baron-Van Evercooren, A., Sotelo, C. and Chedotal, A. (2004). Multiple roles for slits in the control of cell migration in the rostral migratory stream. *J. Neurosci.* **24**, 1497-1506.

Norlin, E. M., Alenius, M., Gussing, F., Hagglund, M., Vedin, V. and Bohm, S. (2001). Evidence for gradients of gene expression correlating with zonal topography of the olfactory sensory map. *Mol. Cell. Neurosci.* **18**, 283-295.

Ogawa, M., Miyata, T., Nakajima, K., Yagyu, K., Seike, M., Ikenaka, K., Yamamoto, H. and Mikoshiba, K. (1995). The reeler gene-associated antigen on Cajal-Retzius neurons is a crucial molecule for laminar organization of cortical neurons. *Neuron* **14**, 899-912.

Oland, L. A., Pott, W. M., Higgins, M. R. and Tolbert, L. P. (1998). Targeted ingrowth and glial relationships of olfactory receptor axons in the primary olfactory pathway of an insect. *J. Comp. Neurol.* **398**, 119-138.

Puche, A. C. and Shipley, M. T. (2001). Radial glia development in the mouse olfactory bulb. *J. Comp. Neurol.* **434**, 1-12.

Raper, J. A. (2000). Semaphorins and their receptors in vertebrates and invertebrates. *Curr. Opin. Neurobiol.* **10**, 88-94.

Ressler, K. J., Sullivan, S. L. and Buck, L. B. (1993). A zonal organization of odorant receptor gene expression in the olfactory epithelium. *Cell* **73**, 597-609.

Sabatier, C., Plump, A. S., Le Ma, Brose, K., Tamada, A., Murakami, F., Lee, E. Y. and Tessier-Lavigne, M. (2004). The divergent Robo family protein rig-1/Robo3 is a negative regulator of slit responsiveness required for midline crossing by commissural axons. *Cell* **117**, 157-169.

Scheffer, I. E., Wallace, R. H., Phillips, F. L., Hewson, P., Reardon, K., Parasivam, G., Stromme, P., Berkovic, S. F., Gecz, J. and Mulley, J. C. (2002). X-linked myoclonic epilepsy with spasticity and intellectual disability: mutation in the homeobox gene ARX. *Neurology* **59**, 348-356.

Seki, T. and Arai, Y. (1993). Highly polysialylated neural cell adhesion molecule (NCAM-H) is expressed by newly generated granule cells in the dentate gyrus of the adult rat. *J. Neurosci.* **13**, 2351-2358.

St John, J. A., Clarris, H. J., McKeown, S., Royal, S. and Key, B. (2003). Sorting and convergence of primary olfactory axons are independent of the olfactory bulb. *J. Comp. Neurol.* **464**, 131-140.

Stout, R. P. and Graziadei, P. P. (1980). Influence of the olfactory placode on the development of the brain in *Xenopus laevis* (Daudin). I. Axonal growth and connections of the transplanted olfactory placode. *Neuroscience* **5**, 2175-2186.

Stromme, P., Mangelsdorf, M. E., Shaw, M. A., Lower, K. M., Lewis, S. M., Bruyere, H., Lutcherath, V., Gedeon, A. K., Wallace, R. H., Scheffer, I. E. et al. (2002). Mutations in the human ortholog of Aristaless cause X-linked mental retardation and epilepsy. *Nat. Genet.* **30**, 441-445.

Sullivan, S. L., Bohm, S., Ressler, K. J., Horowitz, L. F. and Buck, L. B. (1995). Target-independent pattern specification in the olfactory epithelium. *Neuron* **15**, 779-789.

Tomasiewicz, H., Ono, K., Yee, D., Thompson, C., Goridis, C., Rutishauser, U. and Magnuson, T. (1993). Genetic deletion of a neural cell adhesion molecule variant (N-CAM-180) produces distinct defects in the central nervous system. *Neuron* **11**, 1163-1174.

Tsuboi, A., Yoshihara, S., Yamazaki, N., Kasai, H., Asai-Tsuboi, H., Komatsu, M., Serizawa, S., Ishii, T., Matsuda, Y., Nagawa, F. et al. (1999). Olfactory neurons expressing closely linked and homologous odorant receptor genes tend to project their axons to neighboring glomeruli on the olfactory bulb. *J. Neurosci.* **19**, 8409-8418.

Vassar, R., Ngai, J. and Axel, R. (1993). Spatial segregation of odorant receptor expression in the mammalian olfactory epithelium. *Cell* **74**, 309-318.

Wichterle, H., Turnbull, D. H., Nery, S., Fishell, G. and Alvarez-Buylla, A. (2001). In utero fate mapping reveals distinct migratory pathways and fates of neurons born in the mammalian basal forebrain. *Development* **128**, 3759-3771.

Xue, G. P., Calvert, R. A. and Morris, R. J. (1990). Expression of the neuronal surface glycoprotein Thy-1 is under post-transcriptional control, and is spatially regulated, in the developing olfactory system. *Development* **109**, 851-864.

Yoshihara, Y., Kawasaki, M., Tamada, A., Fujita, H., Hayashi, H., Kagamiyama, H. and Mori, K. (1997). OCAM: A new member of the neural cell adhesion molecule family related to zone-to-zone projection of olfactory and vomeronasal axons. *J. Neurosci.* **17**, 5830-5842.